

Quantum Teleportation and Entanglement Swapping for Spin Systems

Dominic W. Berry¹ and Barry C. Sanders^{1,2}

¹*Department of Physics and Centre for Advanced Computing – Algorithms and Cryptography, Macquarie University, Sydney, New South Wales 2109, Australia*

²*Quantum Entanglement Project, ICORP, JST, Edward L. Ginzton Laboratory, Stanford University, California 94305-4085*

(Dated: May 21, 2019)

We analyze quantum teleportation and entanglement swapping for spin systems. If the permitted operations are restricted to a physically realizable interaction, plus local rotations and spin measurements, high-fidelity teleportation is achievable for quantum states that are close to the maximally-weighted spin state. Entanglement swapping is achieved, and is maximized for a combination of entangled states and Bell measurements that is different from the quantum teleportation case. If more general local unitary transformations are considered, then it is possible to achieve perfect teleportation and entanglement swapping.

PACS numbers: 03.67.-a, 03.65.Ud

I. INTRODUCTION

Quantum teleportation (QT) enables disembodied transport of the state of a system to a distant system through (i) a shared entanglement resource, (ii) a classical communication channel between the sender and receiver [1] and (iii) an experimentally established isomorphism between the Hilbert spaces of the sender and receiver [2]. Quantum teleportation is significant for several reasons, including transmission of quantum states in noisy environments [1], sharing states in distributed quantum networks [3] and implementation of quantum computation using resources prepared offline [4, 5]. Teleportation was initially proposed for discrete-variable systems, where the state to be teleported has finite N levels [1], and a continuous-variable (CV) version [6] has been adapted for squeezed light experiments [7]. Our interest here is QT of a quantum state in an arbitrary but finite N -dimensional Hilbert space \mathcal{H}_N , realized physically as a spin system, thereby generalizing the recent spin QT proposal by Kuzmich and Polzik (KP) which is only valid in the infinite- N limit [8].

Entanglement swapping (ES) is closely related to QT. Whereas QT enables the state of a system (e.g. a particle or collection of particles) to be teleported to an independent physical system via classical communication channels and a shared entanglement resource, the purpose of ES is to instill entanglement between systems that hitherto shared no entanglement. An entanglement resource is required for ES to occur; indeed the nomenclature “entanglement swapping” describes the transfer of entanglement from a priori entangled systems to a priori separable systems.

A connection between ES and QT can be seen as follows. Consider QT of the state of one particle, which is initially entangled with a second particle, but the state of the second particle does not undergo QT. In perfect QT the state of the first particle is faithfully transferred to a third particle that was initially independent of the first two particles. Thus, subsequent to the QT, the sec-

ond and third particles are entangled, perfectly replacing the a priori entanglement of the first and second particles. The entanglement resource inherent in QT devices enables this ES to occur; thus, equivalence between optimal entanglement resources for QT and ES might be expected, but we show here that the optimal entanglement resources differ between QT and ES for finite- N spin systems.

Quantum teleportation of states in \mathcal{H}_N can, in principle, be accomplished using the entanglement resource

$$|\Phi\rangle = N^{-1/2} \sum_{m=1}^N |m\rangle \otimes |m\rangle \in \mathcal{H}_N^{\otimes 2} \equiv \mathcal{H}_N \otimes \mathcal{H}_N, \quad (1)$$

by employing the Bell state projective-valued measurement (PVM) $|p, q\rangle\langle p, q|$ [1], where the Bell states are

$$|p, q\rangle = N^{-1/2} \sum_{m=1}^N e^{i2\pi mp/N} |m\rangle \otimes |m + q \bmod N\rangle. \quad (2)$$

These Bell states are mutually orthogonal and are all maximally entangled (see Appendix B for further discussion of these states). This entanglement resource and Bell measurement can also be used to perform ES for multilevel systems by teleportation of entanglement [1].

This PVM does not have an obvious physical realization, however, except for the well-studied case that $N = 2$. On the other hand, we can embed the multilevel system into a spin system, with Hamiltonians expressed as functions of the $\text{su}(2)$ generators J_k , $k \in \{x, y, z\}$, and the irrep is identified by j , with $j(j+1)$ the eigenvalue of the Casimir operator $J^2 = \sum_k J_k^2$ and $2j \in \mathbb{N}$. For given j the corresponding Hilbert space is $\mathcal{H}_{N=2j+1}$. Each subsystem involved in QT and ES has its own conservation of total particle number, hence, j is the same for each subsystem. Thus, the multilevel system to be teleported is regarded as a qudit embedded into an $\text{SU}(2)$ dynamical system [9].

To establish QT of states in \mathcal{H}_N , we adapt the infinite- j limit scheme for QT of spin systems [8] to the case of

finite j , and improve that design for finite- j systems. We identify the optimal two-mode spin-squeezed states for use as an entanglement resource in Sec. II and determine the fidelity of teleportation using this entanglement resource and the Bell measurements of Ref. [8] in Sec. III. We determine the level of ES achieved by this teleportation scheme in Sec. IV and determine a modified interaction that provides significantly improved ES. In Sec. V we identify a Bell state PVM, adapted from that of Sec. IV, such that perfect QT and ES are obtained. Conclusions are presented in Sec. VI.

II. TWO-MODE SPIN-SQUEEZED STATES

One of the three key criteria of QT listed in Sec. I is a shared entanglement resource. In order to establish suitable entangled states, we determine two-mode spin-squeezed states via an optimization scheme and show that these states are indeed entangled. We adapt the KP two-mode spin-squeezed state (subject to a minor transformation of variables equivalent to a permutation of indices for the spin operators) for which the two-mode standard deviations satisfy

$$\Delta J_z^{(+)} \sim 0, \quad \Delta J_y^{(-)} \sim 0. \quad (3)$$

Here $J_k^{(\pm)} = J_k^{(1)} \pm J_k^{(2)}$, for $k \in \{x, y, z\}$. We use the term ‘‘mode’’ to mean the degree of freedom corresponding to each Hilbert space \mathcal{H}_N . Each of the two systems is represented in the same j -irrep; consequently a basis set for two-mode squeezed states is $\{|jm\rangle_z \otimes |jn\rangle_z\} \in \mathcal{H}_{2j+1}^{\otimes 2}$, where $|jm\rangle_z \otimes |jn\rangle_z$ is a simultaneous eigenstate of $J_z^{(1)}$ and $J_z^{(2)}$, with corresponding eigenvalues m and n respectively. An arbitrary state can be expressed as

$$|\Phi\rangle = \sum_{mn} \Phi_{mn} |jm\rangle_z \otimes |jn\rangle_z. \quad (4)$$

In order for the KP teleportation scheme to be effective, it is also necessary that $\langle J_x^{(+)} \rangle \lesssim 2j$. This requirement of proximity to the highest-weight state of $J_x^{(+)}$ requires a compromise with the squeezing condition (3) because decreasing the uncertainties in (3) decreases $\langle J_x^{(+)} \rangle$ as well, by analogy with the single-mode spin-squeezed state counterpart [10, 11]. Restricting to states near the highest-weight state of $J_x^{(+)}$ is equivalent to restricting to states near the $J_x^{(k)}$ highest-weight states for the individual modes $k = 1$ and 2 . This corresponds to working in the Heisenberg–Weyl (HW) limit of SU(2) dynamics, i.e. the dynamics are close to that of a harmonic oscillator [12].

In order to obtain two-mode spin-squeezed states that give high fidelity for the KP teleportation scheme, we need to balance the conflicting criteria of Eq. (3) and $\langle J_x^{(+)} \rangle \lesssim 2j$. This can be done by minimizing the quan-

ity

$$\chi(\mu) = V_z^{(+)} + V_y^{(-)} - \mu \langle J_x^{(+)} \rangle, \quad (5)$$

where $V_z^{(+)}$ and $V_y^{(-)}$ are the variances of $J_z^{(+)}$ and $J_y^{(-)}$ respectively. This optimization gives the minimal variances $V_z^{(+)}$ and $V_y^{(-)}$ for the maximum value of $\langle J_x^{(+)} \rangle$, and the value of μ weights the relative importance of minimizing the variances as compared to maximizing $\langle J_x^{(+)} \rangle$. The optimum value of μ will be found numerically.

It is only possible to minimize χ numerically, as it is fourth order in the state coefficients Φ_{mn} of Eq. (4). We have performed this numerical minimization from random initial states [13] for spins up to $j = 5$, and found that both $\langle J_z^{(+)} \rangle$ and $\langle J_y^{(-)} \rangle$ are equal to zero for the optimal states. We conjecture that $\langle J_z^{(+)} \rangle = \langle J_y^{(-)} \rangle = 0$ for the optimal states for arbitrary spin. This implies that $V_z^{(+)} = \langle (J_z^{(+)})^2 \rangle$ and $V_y^{(-)} = \langle (J_y^{(-)})^2 \rangle$ for the optimal states.

When we make this replacement in Eq. (5), the optimization problem reduces to the minimization of the expectation value of an operator. Using the method of undetermined multipliers, this optimization can be performed by solving the eigenvalue equation

$$\left[(J_z^{(+)})^2 + (J_y^{(-)})^2 - \mu J_x^{(+)} \right] |\nu; \mu\rangle = \nu |\nu; \mu\rangle. \quad (6)$$

This optimization corresponds to determining the state that minimizes $\Delta J_z^{(+)}$ and $\Delta J_y^{(-)}$, with the auxiliary constraint of a fixed value of $\langle J_x^{(+)} \rangle$.

The value of ν can take, in principle, values between $-2j\mu$ and $8j^2 + 2j\mu$. It does not actually reach these bounds, however, because it is not possible to have spectral extrema for all three terms on the left hand side simultaneously. The actual bounds are only determined numerically. The eigenstate corresponding to the minimum eigenvalue ν (i.e. closest to $-2j\mu$) will be the optimal state. In our calculations we have found that this eigenstate is unique, although it is not obvious that this should be the case.

We have performed numerical minimizations of χ , using initial states found by solving the eigenvalue equation (6), for spins up to $j = 20$. These states also minimize χ and satisfy $\langle J_z^{(+)} \rangle = \langle J_y^{(-)} \rangle = 0$. This vindicates our conjecture that $\langle J_z^{(+)} \rangle = \langle J_y^{(-)} \rangle = 0$ for the optimal states.

This optimization procedure is similar to the optimization for the single-mode case considered by Sørensen and Mølmer [11]. They consider the problem of minimizing the variance in J_x for maximal $\langle J_z \rangle$. In their case there is the additional complication that for half-odd integer spin, $\langle J_x \rangle$ is not necessarily zero for the optimal state, whereas we have conjectured and verified numerically that the means are zero in the two-mode case. This complication arises in the single-mode case because J_x has eigenvalues at $\pm 1/2$ but not at zero. It is therefore not possible for the variance of J_x to be less than $1/4$ if the mean is still zero. The minimum uncertainty states

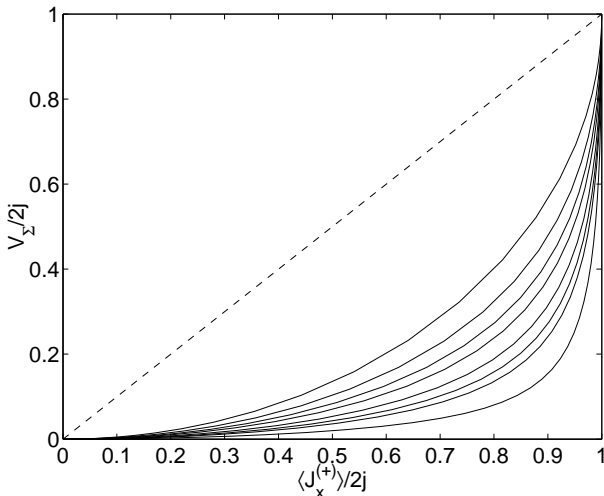


FIG. 1: Variances V_Σ for optimal two-mode spin squeezed states as a function of $\langle J_x^{(+)} \rangle$. In order of decreasing heights, the solid curves correspond to $j = 1/2, 1, 3/2, 2, 3, 4, 5$, and 10 . The dashed line corresponds to $\chi(1) = 0$.

where the variance is less than $1/4$ must be asymmetric with a mean near $\pm 1/2$. On the other hand, for integer spin, J_x has an eigenvalue at zero, and the minimum uncertainty state is symmetric and has zero mean, so the square is the same as the variance. This is equivalent to the result that we find here, because the operators that we wish to minimize, $J_z^{(+)}$ and $J_y^{(-)}$, have integer eigenvalues from $-2j$ to $+2j$, including 0 (regardless of whether the spin j is integer or half-odd integer).

In Fig. 1 the results of optimization by the undetermined multiplier technique are depicted as a graph of the sum of the variances for the optimal state $V_\Sigma \equiv V_z^{(+)} + V_y^{(-)}$ vs the mean $\langle J_x^{(+)} \rangle$. These results are normalized by a factor of $2j$, in order to better compare the results for different j . As can be seen, in order to obtain smaller V_Σ , we require smaller values of $\langle J_x^{(+)} \rangle$. It is possible to obtain a state that satisfies (3) perfectly, i.e. $V_\Sigma = 0$, at the expense of also having $\langle J_x^{(+)} \rangle = 0$. This state,

$$|\mu = 0; \nu = 0\rangle = \frac{1}{\sqrt{2j+1}} \sum_{m=-j}^j |jm\rangle_y \otimes |jm\rangle_y, \quad (7)$$

is maximally entangled and is equivalent to the entanglement resource of Eq. (1) expressed for a two-mode spin system.

Thus far the analysis has been focused on two-mode spin squeezing, whereas the QT requirement is in fact entanglement. The two-mode system is entangled if $\chi(1) < 0$. To see this, recall that the commutation relation $[J_y, J_z] = iJ_x$ implies that $V_y V_z \geq |\langle J_x \rangle|^2 / 4$. In turn this implies that

$$V_z + V_y \geq V_z + \frac{|\langle J_x \rangle|^2}{4V_z} \geq |\langle J_x \rangle|. \quad (8)$$

For unentangled pure states we have $V_z^{(+)} = V_z^{(1)} + V_z^{(2)}$ and $V_y^{(-)} = V_y^{(1)} + V_y^{(2)}$. Note that this does not necessarily hold in the case of a mixed state, as we may have classical correlations. Thus, for unentangled pure states we may add the inequalities (8) for the two modes 1 and 2, giving

$$V_z^{(+)} + V_y^{(-)} \geq |\langle J_x^{(1)} \rangle| + |\langle J_x^{(2)} \rangle| \geq \langle J_x^{(+)} \rangle. \quad (9)$$

Hence $\chi(1) \geq 0$ for unentangled pure states, and $\chi(1) < 0$ implies entanglement. It is also possible to generalize this result to mixed states using the method of Duan *et al.* [14].

The limit below which the states must be entangled, $\chi(1) = 0$, is depicted in Fig. 1 as a dashed line. Except for the end points at $\langle J_x^{(+)} \rangle / 2j = 0$ or 1 , all the results are below this line, demonstrating entanglement. The converse does not hold, however: entanglement does not necessarily imply $\chi(1) < 0$. For example, the maximally entangled state (7) does not satisfy this inequality.

III. QUANTUM TELEPORTATION

In order to perform QT, one share, or mode, of the entanglement resource will be mixed by Alice with the unknown state $|\psi\rangle \in \mathcal{H}_N$ to be teleported in such a way that Alice should learn nothing about the state to be teleported yet obtains classical measurement results (a, b) (via a Bell-type measurement) to share with Bob. Bob receives the results of Alice's measurement via a classical channel. He then performs a unitary transformation based on the result (a, b) on the second mode of the two-mode entangled spin state. Bob's output state, designated $|\zeta_{a,b}\rangle$, should ideally be a replica of the unknown input state $|\psi\rangle$.

The two modes of the entanglement resource are designated 1 and 2, and mode 3 is the state to be teleported. Alice's measurement will take place jointly on modes 2 and 3, and Bob's approximate replica of the original state will be in output mode 1. The Hilbert space for the three modes is $\mathcal{H}_{2j+1}^{\otimes 3}$. KP proposed the measurement corresponding to the nonlinear transformation [8]

$$U = \exp(iJ_y^{(2)} J_z^{(3)}/j), \quad (10)$$

followed by a joint measurement of $J_z^{(2)}$ and $J_y^{(3)}$. Note that we have omitted \otimes in the above expression; we will omit the tensor product symbol from this point on for the sake of brevity.

As mentioned in the previous section, we restrict to entangled states near the maximally weighted J_x eigenstate for modes 1 and 2 (the entanglement resource). Similarly we apply the same restriction to the state to be teleported. By "near" we mean that the state has significant support on the states $|jm\rangle_x$ only for $m \sim j$. For this restriction, we can determine the approximate effect of this unitary transformation using a contraction

to HW(2). To see this, consider the Holstein–Primakoff representation [15]

$$J_0 = j - \hat{n}, \quad J_+ = \sqrt{2j - \hat{n}} a, \quad J_- = a^\dagger \sqrt{2j - \hat{n}}, \quad (11)$$

with

$$J_0 \equiv J_x, \quad J_\pm \equiv J_y \pm iJ_z. \quad (12)$$

The limit we consider here is equivalent to the SU(2)→HW(2) contraction, as considered in Ref. [12], with $\bar{m} \rightarrow j$. The operators have the asymptotic forms

$$J_0 \rightarrow j - a^\dagger a, \quad J_+ \rightarrow \sqrt{2j} a, \quad J_- \rightarrow \sqrt{2j} a^\dagger. \quad (13)$$

In this limit we also find that

$$J_y \rightarrow \sqrt{\frac{j}{2}}(a + a^\dagger) = \sqrt{j} x, \quad (14)$$

$$J_z \rightarrow \frac{1}{i} \sqrt{\frac{j}{2}}(a - a^\dagger) = \sqrt{j} p. \quad (15)$$

Therefore, the unitary transformation (10) becomes

$$U \rightarrow U_{\text{HW}} = \exp(ix^{(2)}p^{(3)}), \quad (16)$$

which generates the displacements

$$\tilde{p}^{(2)} = p^{(2)} + p^{(3)}, \quad \tilde{x}^{(3)} = x^{(3)} - x^{(2)}, \quad (17)$$

where the tildes indicate the transformed variables. Returning to the notation of spin operators, we have the approximate transformation

$$\tilde{J}_z^{(2)} \approx J_z^{(2)} + J_z^{(3)}, \quad \tilde{J}_y^{(3)} \approx J_y^{(3)} - J_y^{(2)}. \quad (18)$$

Let us denote the measured values of $\tilde{J}_z^{(2)}$ and $\tilde{J}_y^{(3)}$ by a and b respectively. The two-mode squeezed state satisfies Eq. (3), hence,

$$\begin{aligned} J_z'^{(1)} &\approx J_z^{(3)} - a, \\ J_y'^{(1)} &\approx J_y^{(3)} - b, \end{aligned} \quad (19)$$

where the prime indicates the operator subsequent to the measurement yielding result (a, b) . Following this measurement, Bob applies the unitary transformation

$$V(a, b) \equiv \exp[i(aJ_y^{(1)} - bJ_z^{(1)})/j], \quad (20)$$

Using the HW(2) contraction, $V(a, b)$ becomes

$$V(a, b) \rightarrow V_{\text{HW}}(a, b) = \exp[i(ax^{(1)} - bp^{(1)})/\sqrt{j}], \quad (21)$$

which gives the transformations

$$\begin{aligned} V_{\text{HW}}^\dagger(a, b)p^{(1)}V_{\text{HW}}(a, b) &= p^{(1)} + a/\sqrt{j}, \\ V_{\text{HW}}^\dagger(a, b)x^{(1)}V_{\text{HW}}(a, b) &= x^{(1)} + b/\sqrt{j}. \end{aligned} \quad (22)$$

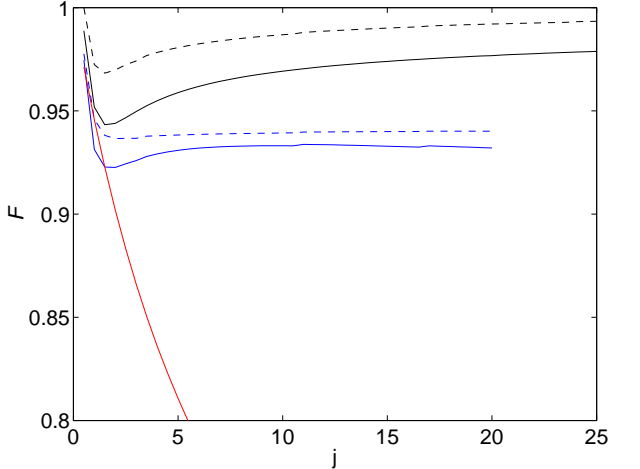


FIG. 2: Fidelity \mathcal{F} for teleportation of $|jj\rangle_x$ states (black lines) and average fidelity \mathcal{F}_{av} over an ensemble of states near $|jj\rangle_x$ (blue lines) as a function of j . The case where the final transformation is as in Eq. (20) is shown as the continuous lines, and that using (25) is shown as the dashed lines. The red line is the approximate maximum fidelity without entanglement.

The approximate transformations of the spin operators are therefore

$$\begin{aligned} V^\dagger(a, b)J_z'^{(1)}V(a, b) &\approx J_z'^{(1)} + a, \\ V^\dagger(a, b)J_y'^{(1)}V(a, b) &\approx J_y'^{(1)} + b. \end{aligned} \quad (23)$$

Therefore, the rotation $V(a, b)$ approximately negates the translations of a and b . This is equivalent to the rotations considered by KP.

Fidelity (A3) is used to characterize the QT of individual states. As discussed in Appendix A, we consider fidelity averaged over the measurement results (a, b) , with weighting according to the probability of obtaining these measurement results. This teleportation protocol is only accurate for input states near the highest-weight eigenstates $|jj\rangle_x$, and it should be most accurate for $|jj\rangle_x$. The fidelity for teleportation of these states is plotted as a function of j in Fig. 2. The entanglement resource is the two-mode spin-squeezed state derived from Eq. (6), with μ optimized to maximize \mathcal{F} for teleportation.

The rotation $V(a, b)$ only approximately negates the terms a and b , and there are many other combinations of rotations that do this. For example, a rotation can be made about the z axis followed by a rotation about the y axis ($e^{iaJ_y^{(1)}/j}e^{-ibJ_z^{(1)}/j}$), or vice versa, or even a sequence of such rotations (e.g. $[e^{iaJ_y^{(1)}/4j}e^{-ibJ_z^{(1)}/4j}]^4$). In general, these rotations are equivalent to a rotation about an axis in the y - z plane (although with slightly different coefficients), plus an additional rotation about the x axis. As there should not be any additional rotation about the x axis, the most accurate teleportation should be for V in the above form: a single rotation about an axis in the y - z plane.

Nevertheless, this argument does not eliminate the possibility that more accurate teleportation may be achieved by using the rotation V with coefficients slightly different from a and b , particularly for the larger values of these two variables. In general, the fidelity should be close to the maximum possible if the orientation of the expectation value of the spin vector for the teleported state is in the same direction as that for the initial state. That is,

$$V^\dagger J'_k V = \gamma \langle J_k^{(3)} \rangle, \quad (24)$$

for some proportionality constant γ and $k \in \{x, y, z\}$. This preservation of orientation can be achieved by using a suitable rotation about an axis in the y - z plane. Unfortunately this rotation will be dependent on the input state, which is in general unknown in QT experiments. To avoid this problem, we determined the rotations for a $|jj\rangle_x$ input state, and applied these rotations to all input states. That is, the rotations V used were those that would give $\langle J_y \rangle = \langle J_z \rangle = 0$ for the output state if the input state were $|jj\rangle_x$. Explicitly this rotation is

$$V(j\xi \langle J_y^{(1)} \rangle, j\xi \langle J_z^{(1)} \rangle), \quad (25)$$

where

$$\xi = \frac{\arccos(\langle J_x^{(1)} \rangle / |\mathbf{J}^{(1)}|)}{\sqrt{\langle J_y^{(1)} \rangle^2 + \langle J_z^{(1)} \rangle^2}}. \quad (26)$$

for

$$|\mathbf{J}^{(1)}|^2 = \langle J_x^{(1)} \rangle^2 + \langle J_y^{(1)} \rangle^2 + \langle J_z^{(1)} \rangle^2. \quad (27)$$

Here the expectation values implicitly depend on the measurement results (a, b) , so these rotations also depend on a and b .

For this scheme of final rotations, the fidelity increases as the entanglement resource is less entangled (for a $|jj\rangle_x$ input state). This higher fidelity does not correspond to better teleportation, as the fidelity is worse for states other than $|jj\rangle_x$. Therefore, rather than separately determining optimum values of μ for the rotations (25), the same values as were determined previously for the $V(a, b)$ rotation were used. The rotations (25) give fidelities significantly higher than those for the simple $V(a, b)$ rotation for $|jj\rangle_x$ states.

In general the quality of a teleportation scheme cannot be judged from the fidelity of teleportation for just one state; we must consider the fidelity as a function of the input state. A good way of quantifying the quality of the teleportation scheme is to determine the average fidelity over an ensemble of states, as in Eq. (A4). Analogously to Ref. [16] for the continuous case, we will take a weighted average over coherent spin states, with weighting function

$$W(|\theta, \phi\rangle) \propto e^{-\theta^2/\sigma}, \quad (28)$$

where σ is approximately the variance for the distribution. The state $|\theta, \phi\rangle$ is a coherent spin state rotated an angle θ away from the x axis, that is

$$|\theta, \phi\rangle = e^{i\phi J_x} e^{i\theta J_y} |jj\rangle_x. \quad (29)$$

These coherent states can alternatively be expressed as

$$|\theta, \phi\rangle = e^{i\theta(J_y \cos \phi - J_z \sin \phi)} |jj\rangle_x. \quad (30)$$

In the limits (13), this becomes

$$|\theta, \phi\rangle \rightarrow e^{i\theta \sqrt{\frac{j}{2}} (e^{i\phi} a + e^{-i\phi} a^\dagger)} |0\rangle = D\left(\theta e^{-i\phi} \sqrt{\frac{j}{2}}\right) |0\rangle, \quad (31)$$

where $|0\rangle$ is the harmonic oscillator vacuum state and $D(\dots)$ is the displacement operator. Thus we see that in this limit the coherent spin states are equivalent to coherent states with coherent amplitude $\theta e^{-i\phi} \sqrt{j/2}$.

Therefore, the probability distribution (28) is analogous to that used in Ref. [16], with $\lambda \equiv 2/\sigma j$. It was found in Ref. [16] that the maximum fidelity without entanglement is $(1 + \lambda)/(2 + \lambda)$. This means that the corresponding limit here is approximately

$$\mathcal{F}_{\max}(\sigma) \approx \frac{1}{2} \frac{\sigma j + 2}{\sigma j + 1}. \quad (32)$$

This will be a good approximation for small σ . Note that this approaches 1/2 in the limit of large j , which is the same as the limit for continuous variable teleportation [16].

The results as determined via numerical integrals, as well as this limit, are depicted in Fig. 2. These results are for the example of $\sigma = (20^\circ)^2$. The average fidelities are still high, well above 0.9, but do not tend to 1 for large spin. Instead they tend towards asymptotic values slightly below 1. Note also that the more sophisticated scheme of final rotations (25) again gives higher fidelity than the simple case $V(a, b)$. The fidelity in both of these cases is well above the limit (32) for spin above about 2. Similar results are obtained for other values of σ , with the average fidelity decreasing as σ is increased.

The explicit variation of the fidelity for coherent spin states rotated by angle θ from the $|jj\rangle_x$ state (i.e. $|\theta, \phi = 0\rangle$ or $|\theta, \phi = \pi/2\rangle$) is shown in Fig. 3. As can be seen, the teleportation is fairly insensitive to rotations about the y axis, with high fidelity for rotations up to 30° or 40° . In contrast the teleportation is more sensitive to rotations about the z axis, with the fidelity dropping off beyond about 20° . This case is for a spin of $j = 20$, but the results are similar for other spins above about 5.

In these figures the fidelity is also compared with two cases where no QT is performed. The first alternative to QT is the fidelity in the limit $\mu \rightarrow \infty$. In this limit the entanglement resource becomes an unentangled $|jj\rangle_x \otimes |jj\rangle_x$ state, so we are constructing the final state based purely on classical measurement results. In this case the fidelity is approximately 50%. The fidelity of teleportation does

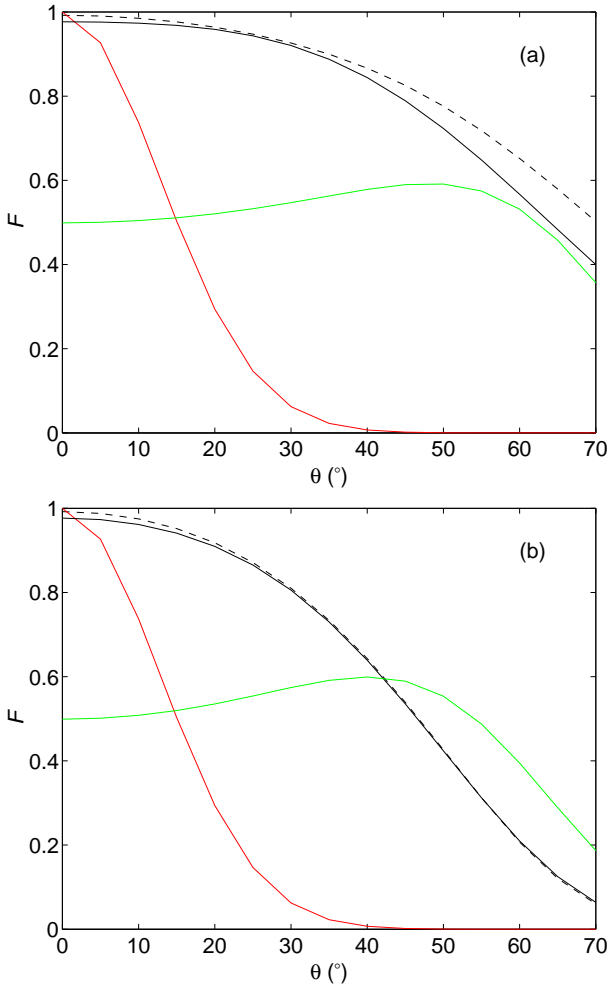


FIG. 3: Fidelity for teleportation of $|jj\rangle_x$ states rotated about the y axis (a) and z axis (b) for $j = 20$. The case for the transformation of Eq. (20) is shown as the continuous black line, and that using (25) is shown as the dashed line. The green line is for no entanglement, and the red line is the fidelity if the output state is always $|jj\rangle_x$.

not fall to this level until quite large rotation angles θ . Note that this result is similar to the result for continuous variable QT [16], where the maximum fidelity with no entanglement resource is 50%. Another (trivial) alternative is where the output state is simply $|jj\rangle_x$, independent of the input state. In this case the fidelity is unity for zero rotation, but quickly falls to very low levels.

A more stringent way of testing the teleportation scheme is to consider input states with nonclassical features. The first example of these that we will consider is single-mode spin squeezed input states. More specifically, the states we will consider are the optimal spin squeezed states as found using a procedure similar to Ref. [11]. The results for the case of spin squeezing in the y direction are shown in Fig. 4 (the results for squeezing in the z direction are not shown as they are almost identical). Again the fidelity for two cases where there is no telepor-

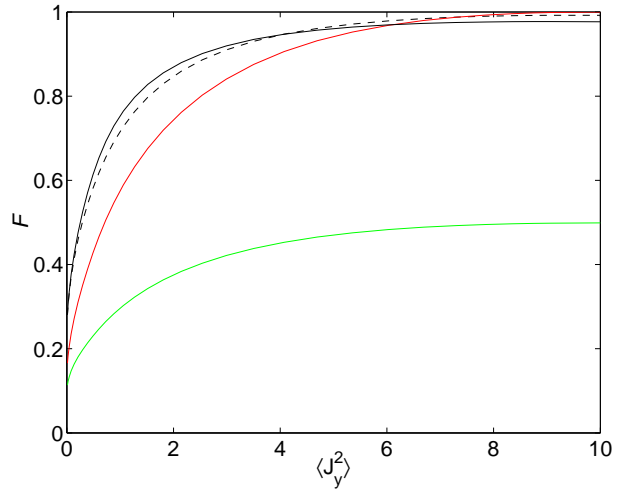


FIG. 4: Fidelity for teleportation of spin squeezed states with reduced fluctuations in J_y for $j = 20$. The case for the transformation of Eq. (20) is shown as the continuous black line, and that using (25) is shown as the dashed line. The green line is for no entanglement, and the red line is the fidelity if the output state is always $|jj\rangle_x$.

tation has been given for comparison. For the case where there is no entanglement, the fidelity is at or below 50%, and well below the fidelity for teleportation. On the other hand, the fidelity for the case where the output state is always $|jj\rangle_x$ closely approximates that for teleportation, except for very high spin squeezing.

As the fidelity for the case where the output state is always $|jj\rangle_x$ is about the same as that for QT, a more sensitive indication of the quality of the teleportation is the spin squeezing in the teleported state. That is because this indicates how much the nonclassical features of the input state have been preserved in the teleportation process. More specifically, we will consider the quantity $V_k = \text{Var}(J_k)$ for spin squeezed states with reduced fluctuations in J_k , $k \in \{y, z\}$. This quantity will be $j/2$ for a coherent spin state, and less for a squeezed spin state. For the output state this quantity was averaged over the detection results, similar to the fidelity. The mean value of V_k for the teleported state is plotted versus the value of V_k for the input in Fig. 5.

In general the degree of squeezing of the teleported state is less than the degree of squeezing in the original state. The preservation of squeezing is markedly worse for low input V_k ; this is because such a squeezed state is far from $|jj\rangle_x$. In the case of squeezing in J_z , Fig. 5 exhibits an enhanced squeezing for input V_k close to $j/2$. This surprising enhancement arises because some of the squeezing that is inherent in the two-mode squeezed resource is transferred into the output state.

Another example of a state with nonclassical features is a superposition of two coherent spin states. Specifically, the states that will be considered are

$$|\psi\rangle = \exp(i\theta J_y)|jj\rangle_x - \exp(-i\theta J_y)|jj\rangle_x. \quad (33)$$

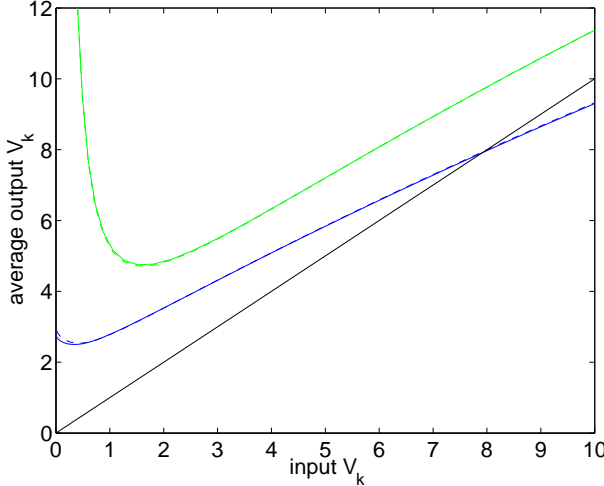


FIG. 5: The mean value of V_k for the output state as a function of V_k for the input state for $j = 20$. The results for the transformation of Eq. (20) are shown as continuous lines, and that using (25) as dashed lines. The results for squeezing in J_y and J_z are shown as the green lines and blue lines respectively. The continuous black line is that for perfect teleportation.

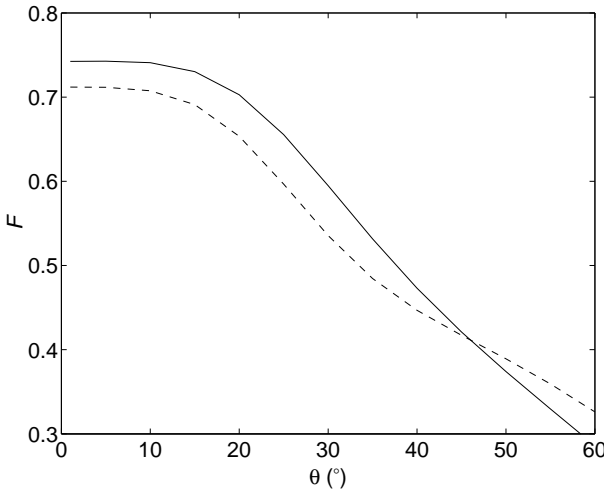


FIG. 6: Fidelity for teleportation of superpositions of coherent spin states for $j = 20$. The case for the transformation of Eq. (20) is shown as the continuous line, and that using (25) is shown as the dashed line.

The variation of the fidelity with θ is plotted in Fig. 6. The fidelity in this case is very poor, for both types of final rotations. Note that the fidelity is larger for smaller rotation angle. The case for zero angle is non-physical ($|\psi\rangle = 0$) and is not plotted. One unusual aspect of these results is that the fidelities for the more complicated rotation (25) are below those for the simple $V(a, b)$ rotation. In contrast the rotation of Eq. (25) generally gives better results for coherent spin states.

In order for this teleportation scheme to be accurate in the limit of large spin, we should expect the fidelity to

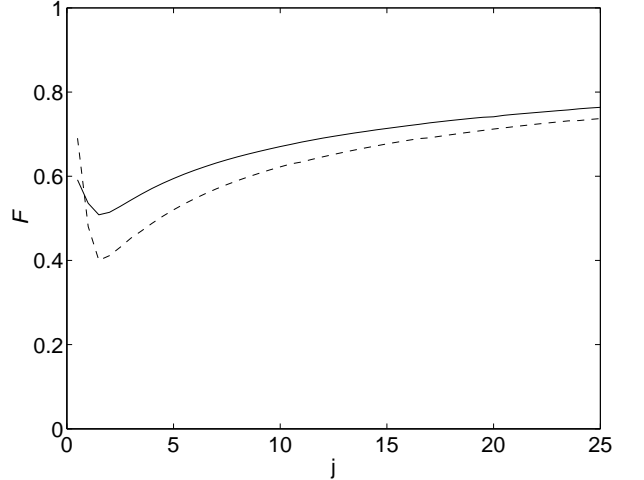


FIG. 7: Fidelity for teleportation of superpositions of coherent spin states for $\theta = 1^\circ$ as a function of j . The case for the transformation of Eq. (20) is shown as the continuous line, and that using (25) is shown as the dashed line.

go to 1 as the spin is increased. The dependence of the fidelity on the spin (for a rotation angle of 1°) is shown in Fig. 7. The fidelity increases with spin for both types of final rotations, but the fidelity is still well below 1 for the largest spin it was feasible to perform calculations for. This low fidelity demonstrates the fragility of a superposition of coherent states under this QT scheme.

IV. ENTANGLEMENT SWAPPING

One way of demonstrating the quantum nature of teleportation is through ES. This is where the state to be teleported (labeled 3), is entangled with another state, which we will label 4. Ideal QT should teleport all properties of the initial state, including entanglement. Therefore, the final teleported state should be entangled with state 4. In the classical case that the final state is reconstructed based on measurement of the initial state with no entanglement resource, there will be no entanglement between the final state and state 4. This means that ES demonstrates that true QT has taken place.

An additional advantage of considering ES over QT is that it is independent of the final transformation applied to the teleported state. This means that it is possible to consider improved Bell measurements without the complication that the fidelity is dependent on the exact final transformation applied.

Firstly we will consider the ES using the teleportation scheme considered in the previous section. The entanglement of formation [17],

$$E = -\text{Tr}(\rho_1 \log_N \rho_1), \quad (34)$$

provides an upper bound for all entanglement measures and is the unique entanglement for a pure state. Similarly

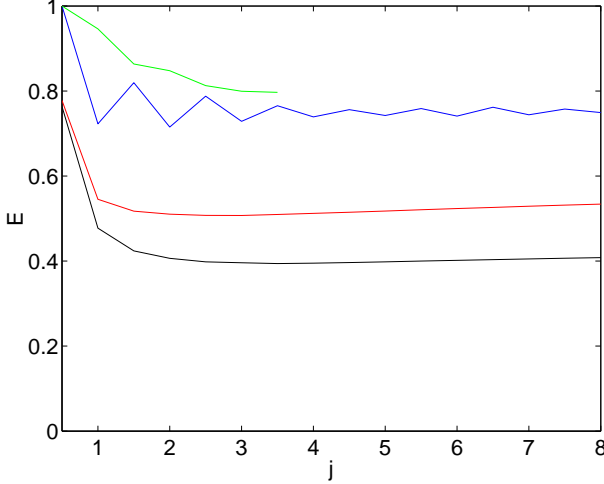


FIG. 8: Entanglement as a function of j . The entanglement swapping using the teleportation scheme of Sec. III is shown as the black line. The coloured lines show results for a maximally entangled entanglement resource and three different interactions U : the results for the interaction of Eq. (10) are shown as the red line, the interaction of Eq. (35) as the blue line, and the interaction of Eq. (36) as the green line.

to the fidelity, the entanglement was averaged over each of the detection results, with weighting according to the probability for obtaining those results.

The average entanglement using the teleportation scheme of the previous section on maximally entangled input states is plotted in Fig. 8. [We do not show additional results for the rotations of Eq. (25), as the final rotations do not affect entanglement.] As can be seen, there is significant entanglement, but the states are far less than maximally entangled. Ideal teleportation would produce perfect entanglement swapping, resulting in the final states being maximally entangled. Nevertheless, the fact that some entanglement swapping takes place convincingly demonstrates the quantum nature of this teleportation scheme.

When we consider entanglement swapping, the values of μ found in the previous section are far from optimum. The maximal final entanglement is achieved for $\mu = 0$, i.e. a maximally entangled entanglement resource. The results for this case are also shown in Fig. 8. As can be seen, the entanglement is significantly higher than for the values of μ used in Sec. III.

It is also possible to improve upon the ES produced by the teleportation scheme of Sec. (III) by considering a modified Bell measurement. The simplest alternative to consider is altering the interaction of Eq. (10) to

$$U = \exp(i\alpha J_y^{(2)} J_z^{(3)}), \quad (35)$$

where α is an arbitrary constant, rather than $1/j$. When the value of α in Eq. (35) is optimized to maximise the final entanglement, the entanglement is as in Fig. 8. The entanglement is significantly greater than that for the

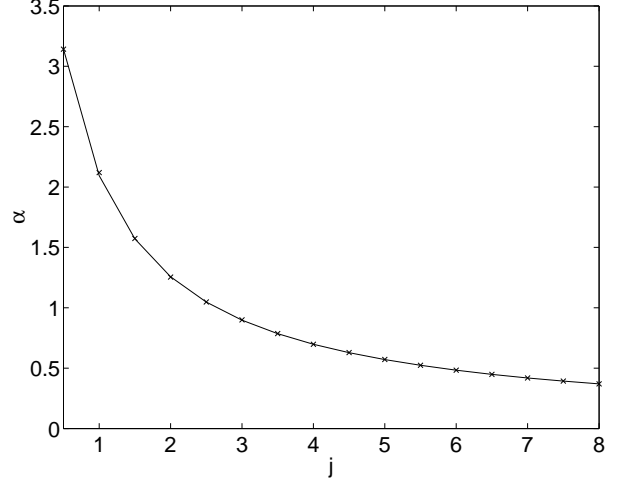


FIG. 9: The optimal values of α as a function of j for the interaction of Eq. (35). The numerical results are shown as the crosses, and the value of $\pi/(j + 1/2)$ is shown as the continuous line.

interaction of Eq. (10), but, except for the case of spin $1/2$, is not unity.

In the case of spin $1/2$ the ES is perfect for $\alpha = \pi$. This value of α also produces perfect QT, provided that the final rotations are $e^{i\pi a J_z^{(3)}} e^{-i\pi b J_y^{(3)}}$. This gives an alternative method to that of Bennett *et al.* for achieving unit fidelity spin $1/2$ teleportation (which is equivalent to that of Bennett *et al.* with the appropriate change of basis).

For $j \geq 1/2$ the optimal values of α are very close to $\pi/(j + 1/2)$ (or $2\pi/N$), as shown in Fig. 9. In fact, for larger spins the optimal values of α are virtually indistinguishable from $\pi/(j + 1/2)$. This indicates that for arbitrary spin we may improve significantly upon the entanglement swapping produced by the KP interaction, simply by changing the value of α from $1/j$ to $\pi/(j+1/2)$.

Another alternative transformation, which is more general, is that given by

$$\begin{aligned} U = & \exp\{i[J_x^{(2)}(\alpha_1 J_x^{(3)} + \alpha_2 J_y^{(3)} + \alpha_3 J_z^{(3)} + \alpha_4 I^{(3)}) \\ & + J_y^{(2)}(\alpha_5 J_x^{(3)} + \alpha_6 J_y^{(3)} + \alpha_7 J_z^{(3)} + \alpha_8 I^{(3)}) \\ & + J_z^{(2)}(\alpha_9 J_x^{(3)} + \alpha_{10} J_y^{(3)} + \alpha_{11} J_z^{(3)} + \alpha_{12} I^{(3)}) \\ & + I^{(2)}(\alpha_{13} J_x^{(3)} + \alpha_{14} J_y^{(3)} + \alpha_{15} J_z^{(3)} + \alpha_{16} I^{(3)})]\}. \quad (36) \end{aligned}$$

Numerically solving for the optimal α_n gives the entanglements shown in Fig. 8. Here results are shown only up to spin $j = 7/2$, as it was not feasible to perform this numerical maximization for larger spin. As can be seen, even allowing this far more general transformation only slightly increases the entanglement.

Unfortunately, although these improved Bell measurements lead to improved ES, they do not necessarily lead to improved fidelity of teleportation. The teleportation theory based on the $SU(2) \rightarrow HW(2)$ contraction does not indicate the appropriate final rotations to perform on the

teleported states for these Bell measurements. Therefore, the final rotations considered were those given by Eq. (25). These rotations should approximately maximize the fidelity for $|jj\rangle_x$, but it was found that even for these input states the fidelity was poor.

V. IDEAL TELEPORTATION

Lastly we will show that it is possible to obtain perfect ES and QT by a minor modification to the above scheme. As is explained in Appendix B, it is possible to perform perfect teleportation using the transformation $e^{\pm i(2\pi/N)\hat{n}^{(2)}\hat{\theta}^{(3)}}$, followed by a joint measurement of $\hat{\theta}^{(2)}$ and $\hat{n}^{(3)}$. Here the operators $\hat{\theta}$ and \hat{n} are canonically conjugate variables, and are equivalent to the operators J_k and θ_k [18] (for $k \in \{x, y, z\}$) in the case of spin.

In the case of spin, we consider the phase eigenstates $\widetilde{|jm\rangle}_k$ for $k \in \{x, y, z\}$, defined by

$$\widetilde{|jm\rangle}_k = N^{-1/2} \sum_{n=-j}^j e^{i2\pi mn/N} |jn\rangle_k, \quad (37)$$

for integer spin, and by

$$\widetilde{|jm\rangle}_k = N^{-1/2} \sum_{n=-j}^j e^{i2\pi(m+\frac{1}{2})(n+\frac{1}{2})/N} |jn\rangle_k, \quad (38)$$

for half-odd integer spin. These definitions are equivalent to those used in Ref. [18], though we are using different notation here. We then define the phase operator θ_k by

$$\theta_k = \sum_{n=-j}^j n \widetilde{|jn\rangle}_k \widetilde{\langle jn|}. \quad (39)$$

This case is slightly different from that considered in Appendix B for half-odd integer spin; however, we still obtain identical results. To see this, consider the Bell states given by Eq. (2), and take the first mode to be J_y eigenstates, and the second mode to be θ_z phase eigenstates. That is, for the first mode

$$|m\rangle \equiv |j, m-j-1\rangle_y, \quad (40)$$

and for the second mode

$$|m\rangle \equiv |j, m-j-1\rangle_z. \quad (41)$$

Using this, the Bell states become, for integer spin

$$|p, q\rangle = \frac{1}{N} \sum_{n,m=-j}^j e^{i2\pi mp/N} e^{i2\pi(m+q)n/N} |jm\rangle_y |jn\rangle_z, \quad (42)$$

and for half-odd integer spin

$$|p, q\rangle = \frac{1}{N} \sum_{n,m=-j}^j e^{i2\pi mp/N} e^{2\pi i(m+q+\frac{1}{2})(n+\frac{1}{2})/N} |jm\rangle_y |jn\rangle_z. \quad (43)$$

In either case the Bell states simplify to

$$|p, q\rangle = e^{i(2\pi/N)J_y^{(2)}J_z^{(3)}} \widetilde{|jp\rangle}_y \widetilde{|jq\rangle}_z. \quad (44)$$

This is the result we obtain using the derivation in Appendix B, with $J_y^{(2)} \equiv \hat{n}^{(2)}$ and $J_z^{(3)} \equiv \hat{\theta}^{(3)}$. Similarly to Appendix B, we can also obtain teleportation using the negative sign in the exponential. We can derive this result from the Bell states in the form

$$|p, q\rangle = N^{-1/2} \sum_{m=1}^N e^{i2\pi mp/N} |m\rangle |q-m \bmod N\rangle, \quad (45)$$

rather than Eq. (2).

These results mean that it is possible to perform these ideal Bell measurements by using the transformation $e^{\pm i(2\pi/N)J_y^{(2)}J_z^{(3)}}$ followed by measurements of $\theta_y^{(2)}$ and $\theta_z^{(3)}$. This is very similar to the result that was found in the previous section, that effective entanglement swapping may be achieved using the transformation $e^{i(2\pi/N)J_y^{(2)}J_z^{(3)}}$, followed by spin measurements.

Thus we find that it is possible to perform perfect teleportation (and therefore ES) that is equivalent to that considered by Bennett *et al.*, by using a slightly different unitary transformation than that considered by KP, and replacing the spin measurements with phase measurements. The modification to the unitary transformation is trivial, and is equivalent to applying the interaction for a longer time. Unfortunately the measurement of phase is nontrivial, and it is not, in general, possible to perform these measurements by simple rotations and spin measurements. The only exception to this is the spin 1/2 case, as the phase eigenstates are also spin eigenstates [9]. This is why it is possible to perform perfect QT and ES in the spin 1/2 case.

Nevertheless, one of the main applications of this quantum teleportation is the transport of states between quantum computers based on qudits. One of the requirements for construction of such a quantum computer is that it is possible to perform arbitrary unitary transformations on a single mode [9]. In that case it is possible to perform phase measurements, simply by performing a unitary transformation between the basis of phase states and the basis of spin states.

It is interesting that the unitary transformation required for perfect teleportation here is distinct from that for the approximate KP teleportation, and does not approach it in the limit of large j . As is shown in Appendix C, the perfect teleportation considered here is equivalent to continuous variable teleportation in the limit of large j . Similarly the teleportation scheme of Sec. III is equivalent to continuous variable teleportation in the limit of large j for states close to the maximally weighted J_x eigenstate. Nevertheless, these limits are fundamentally different, and it does not appear to be possible to perform teleportation that is perfect for arbitrary input states, but is equivalent to KP teleportation for states near $|jj\rangle_x$.

VI. CONCLUSIONS

The KP teleportation scheme provides a physically realizable method of performing teleportation of spin states that are close to $|jj\rangle_x$. Even for moderate photon numbers, high fidelity teleportation is achieved for coherent spin states that are not rotated more than about 20° from $|jj\rangle_x$. The fidelity \mathcal{F}_{av} , averaged over a Gaussian distribution of coherent spin states near $|jj\rangle_x$, is much higher than what is possible without an entanglement resource. The fidelity may be significantly increased for coherent spin states, by using an alternative scheme of final rotations.

This teleportation scheme also teleports the nonclassical features of input states. For input spin-squeezed states, the teleported state also exhibits spin squeezing. In addition, a superposition of two coherent spin states may be teleported, and if the input state is entangled with another state, some of the entanglement will be teleported. The teleportation of these nonclassical features is generally poorer, however. The fidelity for teleportation of a superposition of coherent spin states is poor, except for very large spin and small separation between the two coherent states in the superposition. Also, only about 40% of the entanglement is teleported.

There are improvements that can be made on the ES given by this teleportation scheme. One improvement that can be made is to simply use an optimally entangled entanglement resource. Further improved ES can be obtained by modifying the unitary transformation used for KP Bell measurements from $e^{i(1/j)J_y^{(2)}J_y^{(3)}}$ to $e^{i(2\pi/N)J_y^{(2)}J_y^{(3)}}$. In the case of spin $j = 1/2$, this interaction also allows perfect QT.

If the Bell measurements are further modified by considering phase measurements rather than spin measurements, then it is possible to achieve perfect QT and ES. These Bell measurements are equivalent to those considered by Bennett *et al.* under the appropriate change of basis. Performing phase measurements is non-trivial, and cannot be done using rotations and spin measurements. Nevertheless, if it is possible to perform the more general single-mode unitary transformations required for a quantum computer [9], it should be possible to perform QT in this way.

APPENDIX A: FIDELITY

In this paper we consider three different types of fidelity. The usual definition of fidelity is [19]

$$\mathcal{F} = \langle \psi | \rho | \psi \rangle, \quad (\text{A1})$$

where ρ is Bob's output density operator which can, in general, be mixed. Here we consider Bob's output state $|\zeta_{a,b}\rangle$ to be a pure state that is dependent on the Bell measurement results (a, b) for QT. Using the above definition we obtain a fidelity that is dependent on the input

state $|\psi\rangle$ and the measurement results (a, b)

$$\mathcal{F}(|\psi\rangle, a, b) \equiv |\langle \psi | \zeta_{a,b} \rangle|^2. \quad (\text{A2})$$

We generally do not use this expression as we wish to know the unconditional fidelity, averaged over the measurement results:

$$\mathcal{F}(|\psi\rangle) \equiv \sum_{a,b} P(a, b|\psi) |\langle \psi | \zeta_{a,b} \rangle|^2, \quad (\text{A3})$$

where $P(a, b|\psi)$ is the probability of Alice obtaining the measurement results (a, b) . This expression is equivalent to that considered for schemes without entanglement in Ref. [20].

The fidelity given by Eq. (A3) is applicable only for a specific input state, for which the teleportation is trivial. In general we wish to consider teleportation of a range of states. In this case it is more appropriate to determine the fidelity averaged over this range of states, using

$$\mathcal{F}_{av} = \int W(|\psi\rangle) \left[\sum_{a,b} P(a, b|\psi) |\langle \psi | \zeta_{a,b} \rangle|^2 \right] d\psi, \quad (\text{A4})$$

where $W(|\psi\rangle)$ is the weighting function over the set of states $\{|\psi\rangle\}$. We use the differential $d\psi$ to indicate an integral over the state coefficients with the additional constraint that the state is normalized, i.e.

$$d\psi \equiv \delta(|\langle \psi | \psi \rangle| - 1) d^{2N}(\langle m | \psi \rangle), \quad (\text{A5})$$

where $|m\rangle$ is a basis state of \mathcal{H}_N as used in Eq. (2). In this study, we consider a weighted average over coherent spin states; that is

$$\mathcal{F}_{av} = \int W(|\theta, \phi\rangle) \left[\sum_{a,b} P(a, b|\theta, \phi) |\langle \theta, \phi | \zeta_{a,b} \rangle|^2 \right] d\Omega, \quad (\text{A6})$$

where $d\Omega$ is a unit of solid angle and $|\theta, \phi\rangle$ is a coherent spin state, as in Eq. (29).

APPENDIX B: BELL STATES

We can consider Bell states slightly more general than those of Bennett *et al.* (2), of the form

$$|p, q, s_1, s_2, s_3\rangle = N^{-1/2} \sum_{m=1}^N e^{is_1 2\pi mp/N} |m\rangle |s_2 m + s_3 q\rangle, \quad (\text{B1})$$

where the variables s_k , $k \in \{1, 2, 3\}$ take the values ± 1 , and the modulo N has been omitted for brevity. Each of these states is maximally entangled, and states for differing p or q are orthogonal. Now we define the conjugate states

$$\widetilde{|m\rangle} = N^{-1/2} \sum_{n=1}^N e^{is_2 2\pi mn/N} |n\rangle. \quad (\text{B2})$$

For additional generality we have included the signs s_k . We will use the subscripts $k = 4$ and 5 for modes 2 and 3 , respectively. The states $|m\rangle$ and $|\widetilde{n}\rangle$ satisfy the conjugacy relation

$$\langle m|\widetilde{n}\rangle = N^{-1/2}e^{is_k2\pi mn/N}, \quad (\text{B3})$$

analogous to the conjugacy relation between position and momentum eigenstates, $|x\rangle$ and $|p\rangle$, respectively:

$$\langle x|p\rangle = (2\pi)^{-1/2}e^{ixp}, \quad (\text{B4})$$

where we have taken $\hbar = 1$. By using the inverse relation to (B2) on mode 3 ,

$$|n\rangle = N^{-1/2} \sum_{n=1}^N e^{-is_52\pi mn/N} |\widetilde{m}\rangle, \quad (\text{B5})$$

we obtain

$$\begin{aligned} & |p, q, s_1, s_2, s_3\rangle \\ &= \frac{1}{N} \sum_{n,m=1}^N e^{is_12\pi mp/N} e^{-is_52\pi n(s_2m+s_3q)/N} |m\rangle |\widetilde{n}\rangle. \end{aligned} \quad (\text{B6})$$

This can be expressed as

$$|p, q, s_1, s_2, s_3\rangle = e^{-is_5s_22\pi\hat{n}^{(2)}\hat{\theta}^{(3)}/N} |\widetilde{s_4s_1p}\rangle |s_3q\rangle, \quad (\text{B7})$$

where the operators \hat{n} and $\hat{\theta}$ denote the operators corresponding to the states $|n\rangle$ and $|\widetilde{n}\rangle$ respectively, the superscripts (2) and (3) indicate operators on the first and second modes respectively, and the modulo N has been omitted from the states for brevity.

This demonstrates that perfect teleportation can be achieved by performing the transformation $e^{\pm\frac{2\pi i}{N}\hat{n}^{(2)}\hat{\theta}^{(3)}}$, followed by a joint measurement of $\hat{\theta}^{(2)}$ and $\hat{n}^{(3)}$. Note that the sign in this transformation is arbitrary, and does not depend on the signs used in transforming between the conjugate states, as there is the additional sign s_2 . In more general terms, teleportation is achieved when the operators in the interaction are conjugate to those that are measured.

APPENDIX C: LARGE N LIMIT

Considering the Bell states given by Eq. (2), it is clear that the result q is equivalent to the result of a measurement of $\hat{n}^{(3)} - \hat{n}^{(2)}$ modulo N . It is possible to reexpress

the Bell states (2) as

$$|p, q\rangle = N^{-1/2} \sum_{m=1}^N e^{-i2\pi nq/N} |\widetilde{p-n}\rangle |\widetilde{n}\rangle, \quad (\text{C1})$$

where the modulo N has again been omitted for brevity. Here we are using the conjugate states as in the previous section with $s_k = 1$, $k \in \{4, 5\}$. From this form of the Bell states, it is clear that p is equivalent to a measurement of $\hat{\theta}^{(2)} + \hat{\theta}^{(3)}$ modulo N .

Thus we find that the Bell measurements are equivalent to a joint measurement of $\hat{n}^{(3)} - \hat{n}^{(2)}$ and $\hat{\theta}^{(2)} + \hat{\theta}^{(3)}$ modulo N . In addition, the entangled state is equivalent to an eigenstate of $\hat{n}^{(2)} - \hat{n}^{(1)}$ and $\hat{\theta}^{(1)} + \hat{\theta}^{(2)}$ modulo N . This is very similar to the case of teleportation of continuous variables [6].

Let us make the substitutions

$$\hat{x}_N = \sqrt{\frac{2\pi}{N}} \hat{n}, \quad \hat{p}_N = \sqrt{\frac{2\pi}{N}} \hat{\theta}. \quad (\text{C2})$$

The eigenvectors for these variables satisfy

$$\langle x_N|p_N\rangle = N^{-1/2}e^{ix_Np_N}, \quad (\text{C3})$$

which is equivalent to that for position and momentum, apart from a multiplying factor. In the limit $N \rightarrow \infty$, the ranges of x_N and p_N go to infinity, while the spacing between the eigenvalues goes to zero, so these variables are equivalent to continuous position and momentum. In this limit, it is clear that the teleportation is equivalent to the teleportation considered in [6].

ACKNOWLEDGMENTS

We gratefully acknowledge valuable discussions with S. D. Bartlett. This research was supported by the Australian Research Council.

[1] C. H. Bennett, G. Brassard, C. Crepeau, R. Jozsa, A. Peres, and W. K. Wootters, Phys. Rev. Lett. **70**, 1895 (1993).
[2] S. J. van Enk, quant-ph/0102004.
[3] J. I. Cirac, A. K. Ekert, S. F. H. Huelga and C. Macchiavello, Phys. Rev. A **59**, 4249 (1999).
[4] D. Gottesman and I. L. Chuang, Nature **402**, 390 (1999).
[5] E. Knill, R. Laflamme and G. J. Milburn, Nature **409**,

46 (2001).

[6] L. Vaidman, Phys. Rev. A **49**, 1473 (1994).

[7] S. L. Braunstein and H. J. Kimble, Phys. Rev. Lett. **80**, 869 (1998); A. Furusawa *et al.*, Science **282**, 706 (1998).

[8] A. Kuzmich and E. S. Polzik, Phys. Rev. Lett. **85**, 5639 (2000).

[9] S. D. Bartlett, H. de Guise, B. C. Sanders, and B. T. H. Varcoe, quant-ph/0011080.

[10] M. Kitagawa and M. Ueda, Phys. Rev. A **47**, 5138 (1993).

[11] A. S. Sørensen and K. Mølmer, Phys. Rev. Lett. **86**, 4431 (2001).

[12] D. J. Rowe, H. de Guise, and B. C. Sanders, J. Math. Phys. **42**, 2315 (2001).

[13] The initial random state is assumed to have real coefficients Φ_{mn} that are selected from independent normal distributions, centred at zero for each (m, n) , with the constraint that the state $|\Phi\rangle$ is normalized.

[14] L. M. Duan, G. Giedke, J. I. Cirac, and P. Zoller, Phys. Rev. Lett. **84**, 2722 (2000).

[15] T. Holstein and H. Primakoff, Phys. Rev. **58** 1098 (1940).

[16] S. L. Braunstein, C. A. Fuchs, and H. J. Kimble, J. Mod. Opt. **47**, 267 (2000).

[17] M. Horodecki, P. Horodecki, and R. Horodecki, Phys. Rev. Lett. **84**, 2014 (2000).

[18] A. Vourdas, Phys. Rev. A **41**, 1653 (1990).

[19] B. Schumacher and M. A. Nielsen, Phys. Rev. A **54**, 2629 (1996).

[20] L. Henderson, L. Hardy, and V. Vedral, Phys. Rev. A **61**, 062306 (2000).